Chemosphere 341 (2023) 140110

Contents lists available at ScienceDirect

Chemosphere

journal homepage: www.elsevier.com/locate/chemosphere

Screening of tolerance of Atriplex vulgatissima under zinc or lead experimental conditions. An integrative perspective by using the integrated biological response index (IBRv2).

María de la Paz Pollicelli [a,b], Federico Márquez [b,c], María Débora Pollicelli [b,d], Yanina L. Idaszkin [a,b,*]

[a] Instituto Patagónico para el Estudio de los Ecosistemas Continentales (IPEEC-CONICET), Boulevard Brown 2915, U9120ACD Puerto Madryn, Chubut, Argentina
[b] Universidad Nacional de la Patagonia San Juan Bosco, Boulevard Brown 3051, U9120ACD Puerto Madryn, Chubut, Argentina
[c] Instituto de Biología de Organismos Marinos (IBIOMAR-CONICET), Boulevard Brown 2915, U9120ACD Puerto Madryn, Chubut, Argentina
[d] Centro Para el Estudio de Sistemas Marinos (CESIMAR-CONICET), Boulevard Brown 2915, U9120ACD Puerto Madryn, Chubut, Argentina

HIGHLIGHTS

- *Atriplex vulgatissima* was subjected to different Pb and Zn rises.
- Physiological and biochemical responses showed different behaviour according to metal.
- Both Pb and Zn induced similar morphometric changes in leaves.
- Integrated biological index showed that 200 μM Zn was the most affected treatment.
- *A. vulgatissima* is suitable for Pb phytostabilization and Zn phytoextration.

GRAPHICAL ABSTRACT

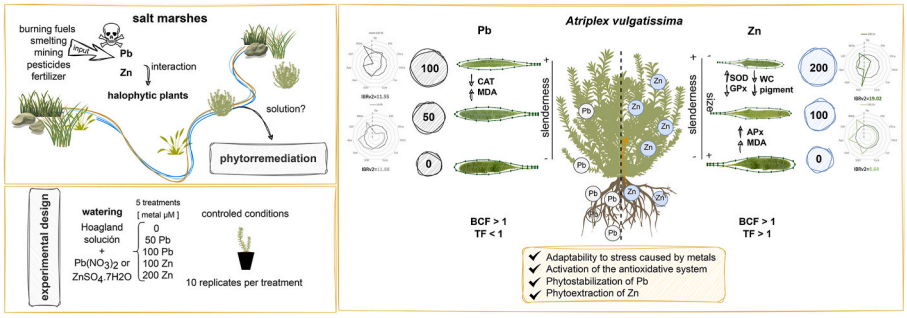

ARTICLE INFO

Handling editor: T Cutright

Keywords:
Atriplex vulgatissima
Lead
Zinc
Phytoremediation
Biomarkers
IBRv2

ABSTRACT

The search for plants with a high capacity to tolerate and accumulate metals is an important issue in phytoremediation. In this sense, this study was conducted in the halophyte *Atriplex vulgatissima* to evaluate the effects of different concentrations of lead (Pb, 50 and 100 μM) or zinc (Zn, 100 and 200 μM) on morphological, physiological, and biochemical parameters as well as the accumulation patterns of this species. The results indicated that while essential metal Zn showed high translocation from roots to shoots (TF > 1), non-essential Pb was mainly accumulated in the roots (BCF>1). Regarding shape, both metals induced slenderness of the blade, but only Zn treatment reduced leaf size. No difference in biomass production and photosynthetic parameters was found between Pb and Zn treatments. Pb treatments did not show significant differences between treatments regarding water content (WC), pigment concentration, and the activity of superoxide dismutase (SOD) and guaiacol peroxidase (GPx), but did result in a decrease in catalase activity at 100 μM Pb. On the other hand, 200 μM Zn leads to a clear reduction in WC and pigment concentrations, along with an increase in SOD and GPx activities. In addition, ascorbate peroxidase (APx) activity showed a hormesis effect at 50 μM Pb and 100 μM Zn.

* Corresponding author. Instituto Patagónico para el Estudio de los Ecosistemas Continentales (IPEEC-CONICET), Boulevard Brown 2915, U9120ACD Puerto Madryn, Chubut, Argentina.
E-mail address: idaszkin@cenpat-conicet.gob.ar (Y.L. Idaszkin).

https://doi.org/10.1016/j.chemosphere.2023.140110
Received 24 May 2023; Received in revised form 1 September 2023; Accepted 6 September 2023
Available online 8 September 2023

Malondialdehyde increased with both Pb and Zn treatments. The integrated biological index (IBRv2) indicated that 200 μM Zn was the most affected treatment (IBRv2 = 19.02) and that under the same concentrations of metals (100 μM Pb or Zn), Pb treatments presented major stress (IBRv2 = 11.55). *A. vulgatissima* is a metallophyte with the potential for Pb phytostabilization and Zn phytoextraction, as well as a bioindicator of these metals. Its high biomass and deep roots, combined with its halophytic traits, make it suitable for bioremediation and monitoring programs.

1. Introduction

Salt marshes are ecosystems with great ecological value (Anjum et al., 2014). Despite their inherent importance, salt marshes have been increasingly subjected to several pollutants from anthropogenic activities, modified and destroyed. Among them, metals are one of the most hazardous, persistent, and non-biodegradable pollutants damaging and risking these environments (Saxena et al., 2020; Roe et al., 2021). In particular, lead (Pb) and zinc (Zn) often occur concomitantly in many polluted areas (Brunetti et al., 2009; Hasnaoui et al., 2020; Alam et al., 2023). Anthropogenic practices such as smelting, mining, burning of fossil fuels, and using pesticides and fertilizers are some contaminating main sources of these metals. Pb is a non-essential metal for plants, resulting toxic at low concentrations and affecting various physiological and biochemical pathways. It can suppress plant growth, inhibit and damage the structure and function of photosystem II, as well as affecting chlorophyll production and the antioxidant system (Zulfiqar et al., 2019). On the other hand, although Zn is a micronutrient implicated in several metabolic functions, it is highly toxic at elevated concentrations and produces biochemical, physiological, and morphological damage (Balafrej et al., 2020; Kaur and Garg, 2021).

Halophyte plants possess adaptive mechanisms (exclusion, sequestration, and exudation of ions and metabolic adjustment) that confer a coupled tolerance to metals (Van Osten and Maggio, 2015; Aziz and Mujeeb, 2022; Singh et al., 2023). Metals, such as Pb and Zn, can induce the production and accumulation of reactive oxygen species (ROS). In this way, halophytes have developed an effective antioxidant system for removing and alleviating the ROS effect (Grigore and Toma, 2021). Among them, superoxide dismutase (SOD), catalase (CAT), ascorbate peroxidase (APx), and guaiacol peroxidase (GPx) are some enzymes that prevent harmful effects in cells, including lipid peroxidation. Furthermore, inhibiting synthesis and reducing chlorophyll and carotenoid content are other consequences of exposure to these metals (Zulfiqar et al., 2019; Kaur and Garg, 2021). When the defense system cannot counter metal effects, the damage could be manifest and detected at several levels: morphological, physiological, biochemical, and/or genomic. These responses, namely biomarkers, are increasingly used in biomonitoring programs because they allow the detection of pollution early and at a low cost (Milinkovitch et al., 2019).

One of the biggest challenges in monitoring and bioremediation programs is the difficulty in summarizing, integrating, and interpreting these individual biomarker responses. In this sense, different multibiomarkers indices have been developed over the last few decades and employed to assess ecosystem health and to detect metal stress on organisms, obtaining a global picture of the polluted sites (Beliaeff and Burgeot, 2002; Lomartire et al., 2021; Truchet et al., 2023). Sanchez et al. (2013) proposed the novel index "Integrative Biomarker Response version 2" (IBRv2), which is based on the deviation concept and could be used not only in large-scale monitoring programs but also in up- and downstream investigation.

The genus *Atriplex* contains between 250 and 300 species, distributed worldwide inhabiting arid and semi-arid environments, and includes herbs and shrubs with abundant foliar biomass and deep root systems adapted to poor and polluted substrates, as well as drought and salinity of coastal habitats (Kumari et al., 2019; Čalasan et al., 2022). Several species of this genus have been described as potential phytoremediators due to their high capacity to tolerate and accumulate metals (Kachout et al., 2010, 2023; Manousaki and Kalogerakis, 2011; Mesnoua et al., 2016; Bankaji et al., 2019; Laghlimi et al., 2022). Particularly, *Atriplex vulgatissima* Speg. (Chenopodiaceae) is a C4 perennial native shrub distributed along Southern Argentina (Neuquén, Chubut, and Santa Cruz) and Central Chile (Brignone et al., 2016). Like other *Atriplex* species, this saltbush has high biomass production, a deep root system, and the capacity to tolerate salt marsh stressors.

Phytoremediation is an ecological and cost-effective alternative that uses plants to remove contaminants through different processes (Ali et al., 2013; Shen et al., 2022; Yang et al., 2022). When plants translocate and concentrate metals in their aboveground tissues, above certain levels, they could be used for phytoextraction. On the other hand, if plants mostly immobilize metals in their belowground tissues or induce precipitation of metals in the rhizosphere, they are suitable for phytostabilization, preventing their off-site movement (Caparrós et al., 2022). The success of phytoremediation requires a clear understanding of some biological aspects of the species to be used (*e.g.*, metal tolerance limits, accumulation capacity, and mechanisms to improve the tolerance). Due to the gap in knowledge of *A. vulgatissima* as a potential phytoremediator and bioindicator of metals, the aims of this study were: I) to assess the effect of Pb and Zn addition on *A. vulgatissima* through the use of biochemical, physiological, and morphological biomarkers; II) to determine the capacity of *A. vulgatissima* to accumulate Pb and Zn; and III) to evaluate the effect of Pb and Zn on *A. vulgatissima* through the calculation of IBRv2 integrally.

2. Materials and methods

2.1. Plant material and experimental setup

Seeds of *A. vulgatissima* were collected in April 2019 from the Riacho salt marsh (Península Valdés, Chubut, Argentina). After storage at 4 °C, they were removed from the bracts and germinated in Petri dishes with deionized water. The seedlings were transferred separately into inert pearlite-filled pots (one plant per pot) and incubated under growth chamber conditions, with a light/dark regime of 16 h at 25 °C/8 h at 15 °C, respectively. After eight months, plants were randomly divided into five groups (n = 10 per treatment) to start the experimental phase. One group per tray was assigned to one of the five treatments: 50 and 100 μM Pb, 100 and 200 μM Zn, and the control treatment (without Pb and with minimal Zn content in Hoagland solution as an essential trace nutrient). The selection of Pb and Zn concentrations was determined by considering the levels of bioavailable soil metals in a Patagonian salt marsh, as reported by Pollicelli et al. (2018), and taking into account findings from other experimental studies (Wu et al., 2013; Dresler et al., 2017; Idaszkin et al., 2019, 2023). During the experiment (six weeks), treatments were irrigated with 1 L of Hoagland solution with the corresponding amount of Pb $(NO_3)_2$ or $ZnSO_4.7H_2O$. The Hoagland solution was used between irrigations to prevent plants from drying and to avoid variations of Pb and Zn concentrations due to water evaporation. Moreover, all the solution in each tray was changed weekly.

2.2. Leaves collection and data acquisition for morphometric analyses

At the end of the experiment, the six new fully expanded leaves were sampled from two branches of each plant of all treatments (n = 60) from the petiole base, maintaining a homology criterion in the procedure.

These leaves were pressed, dried, and scanned at 600 dpi using a conventional scanner Epson Perfection v37 ®, to obtain the image of the adaxial side of each leaf.

Geometric morphometric data were obtained following the procedure as detailed in Idaszkin et al. (2019), through the application of TPS series modules. The overall leaf shape was defined through 5 landmarks and 20 semi-landmarks (Fig. 1), using the tpsDig2 module of the TPS series (Rohlf, 2017a). A total of 300 leaves were digitized, and 19 leaves were excluded for damaged visible or broken outlines. Moreover, the possible differences arising from the arching effects of each leaf were correct through the longitudinal axis defined for landmarks 1, 24, and 25, using the function "unbend specimens" in the module tpsUtil v1.58 (Rohlf, 2017b). After that, landmark 25 was deleted. All semi-landmarks were slid along the outline profile of the leaf using the module of tpsRelw v 1.64 (Rohlf, 2017c) that employs the minimum bending energy criterion (Gunz et al., 2005).

2.3. Growth, physiological and biochemical parameters

At the end of the experiment, a total of 0.7 g of a fresh leaf was randomly sampled (n = 5 per treatment), fixed in liquid N_2, and stored (at −80 °C) in separate bags (0.1, 0.3, and 0.3 g) until biochemical determinations (see below). After that, all plants were harvested and divided into shoot and root systems. The harvest was meticulously rinsed with distilled water to remove perlite and particles attached to plant surfaces and weighed to register fresh weight (FW). Then harvest was dried at 45 °C until constant weight to calculate the final dry biomass (DM) and use it for metals quantification (see below).

The water content in shoots for each treatment was estimated according to Jin et al. (2017) as the difference between fresh and dry weight using formula (1):

$$WC\ (\%) = (FW - DW)/\ FW*100$$

Before the harvest, fluorescence parameters were randomly measured on new fully expanded leaves (n = 5 per treatment, one measurement per plant) using a portable chlorophyll meter FluorPen FP100 (Photon Systems Instruments, Drasov, Czech Republic). Light- and dark-adapted (for 30 min) fluorescence parameters were measured from the same leaf section of each plant (Pérez-Romero et al., 2018). Values of F_0/F'_0 and F_m/F'_m were employed to calculate the maximum quantum efficiency of PSII photochemistry by mean of formula (2):

$$Qy = (F_m - F_0)/\ F_m$$

and the quantum efficiency of PSII was calculated using the following formula (3):

$$\Phi psII = (F'_m - F'_0)/\ F'_m$$

Where F_0 is the minimal fluorescence, F'_0 is the minimal fluorescence in leaves illuminated with far-red light, F_m is the maximum fluorescence, and F'_m is the maximum fluorescence in illuminated leaves (Maxwell and Johnson, 2000).

For the quantification of pigments, 0.1 g leaf material was freeze-dried for 48 h in the dark to avoid photodegradation. Then, each sample was crushed and homogenized with 10 ml of 80% acetone, stored at 4 °C for 1 h, and centrifuged at 5000 rpm for 5 min at 4 °C. The supernatants were collected to determine chlorophyll *a*, *b*, and carotenoid content by using three different wavelengths: 470, 646.8, and 663.2 nm. The concentrated pigments were calculated according to Lichtenthaler (1987).

For enzyme extraction, 0.3 g leaf material was homogenized in 4 ml of 50 mM sodium phosphate buffer (pH 7.6) containing 0.1 mM Na-EDTA. The homogenates were centrifuged at 8923 rpm for 20 min at 4 °C, and the resulting supernatant was used for reaction mixture and subsequent enzyme determinations. Superoxide dismutase (SOD) activity was determined according to Marklund and Marklund (1974) by recording the pyrogallol reduction at 325 nm. Catalase (CAT) activity was estimated by monitoring the decrease in absorbance at 240 nm due to the consumption of H_2O_2, according to Teranishi et al. (1974). Ascorbate peroxidase (APx) activity was performed according to Tiryakioglu et al. (2006) by following the decrease in absorbance at 290 nm. Guaiacol peroxidase (GPx) activity was determined by monitoring the increment of absorbance at 470 nm following the method of Bergmeyer et al. (1974). The results of activity measurements were expressed as U per min per g of fresh weight.

Lipid peroxidation was determined by measuring malondialdehyde (MDA) content using the thiobarbituric acid reactive substances (TBARs) spectrometric method, following the protocol of Heath and Packer (1968). Samples (0.3 g) were homogenized in 3 ml of a solution containing 20% trichloroacetic acid and 0.5% thiobarbituric acid. Homogenates were heated in a boiling water bath at 95 °C for 30 min and immediately cooled in ice for 15 min. After that, they were centrifuged at 4930 rpm for 5 min at 4 °C, and the supernatant absorbance was measured at 532 and 600 nm. The MDA concentration was obtained by applying the extinction coefficient of 155 $nM^{-1}\ cm^{-1}$.

2.4. Pb and Zn accumulation in plant tissues

Sub-samples of 0.5 g of dried and ground roots and shoots were digested separately with 10 ml of concentrate HNO_3 for 10 min using a microwave *Nova*WAVE SA (n = 5 per treatment). Then, they were diluted to a final volume of 45 ml with ultrapure water. Metal concentrations were determined via inductively coupled plasma atomic emission spectroscopy (ICP-AES Agilent 720).

To evaluate accumulation patterns and the efficiency of metal accumulation by plants, we calculated the bioconcentration factor (BCF) = [metal concentration in root]/[metal concentration in solution] and the translocation factor (TF) = [metal concentration in shoot]/[metal concentration in root].

2.5. Integrated biological response index

To summarize and integrate the information of all biomarkers in a single value and graph the IBRv2 index was calculated (Sanchez et al., 2013) using the function *ibrv2_index* of the *IBRtools* package (Resende et al., 2022). This index is independent of the arrangement of the biomarkers on the star plot and is based on the concept of reference deviation between undisturbed and disturbed states. We used the control treatment as a reference level. The area above the control treatment indicates biomarker induction and the area below the control reflects

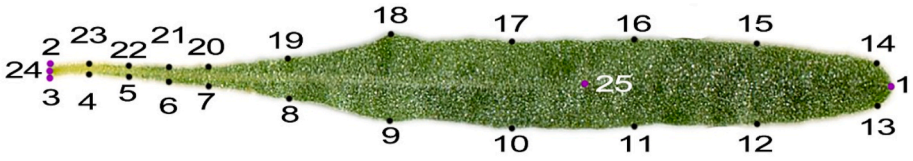

Fig. 1. Configuration of landmarks (violet dots) and semi-landmarks (black dots) on the contour of the leaf of *A. vulgatissima* Landmarks (•): (1) apex, (2) left tip of the petiole, (3) right tip of petiole, (24) middle point between landmarks 2 and 3, and (25) centroid of the blade on midrib. Semilandmarks (•): (4–13; 14–23) along the contour of blade and petiole.

biomarker inhibition.

2.6. Statistical analyses

A Generalized Procrustes Analysis (GPA), which eliminates the effect of translation, rotation, and scale, was performed using the software TpsRelw (Dryden and Mardia, 1998; Klingenberg et al., 2002; Rohlf, 2017c). Then, the centroid size (CS) of leaves was calculated, defined as the square root of the sum of the squared distances from the landmarks to the centroid, and it was used as a proxy for size. The pure shape information was preserved as aligned specimens and exported to MorphoJ software (Klingenberg, 2011) along with the CS values for the statistical shape analysis. The shape analyses were performed on the symmetric component of shape (Klingenberg, 2011) and the allometric effect was assessed by multivariate regression of shape (aligned Procrustes coordinates) on CS; statistical significance was evaluated through a permutation test with 10000 iterations. A canonical variance analysis (CVA) was performed using the average of six leaves per plant to determine the leaf shape components that maximize the differences among treatments (n = 10 per treatment).

Non-geometric morphometric data were subjected to analysis of variance (ANOVA) to test the effects of metals separately (Pb or Zn as fixed factors) on all response variables using the Generalized Least Squares model (GLS). For those variables with a Gaussian distribution of residuals, the *gls* function of the *nlme* package was used. GLS model assumptions were verified by graphical examination of the residuals and by testing for normality (Shapiro–Wilk test) and homogeneity of variances (Levene's test). To model variance heterogeneity among treatments for variables WC, MDA, and metal concentration, the function *VarIdent* in the *nlme* package was used (Pinheiro and Bates, 2006). Tuckey's tests were used for multiple posterior comparisons only when ANOVA resulted in significative ($P \leq 0.05$) (Zar, 1999). All statistical analyses were performed in R v4.0.1 (R Core Team, 2023).

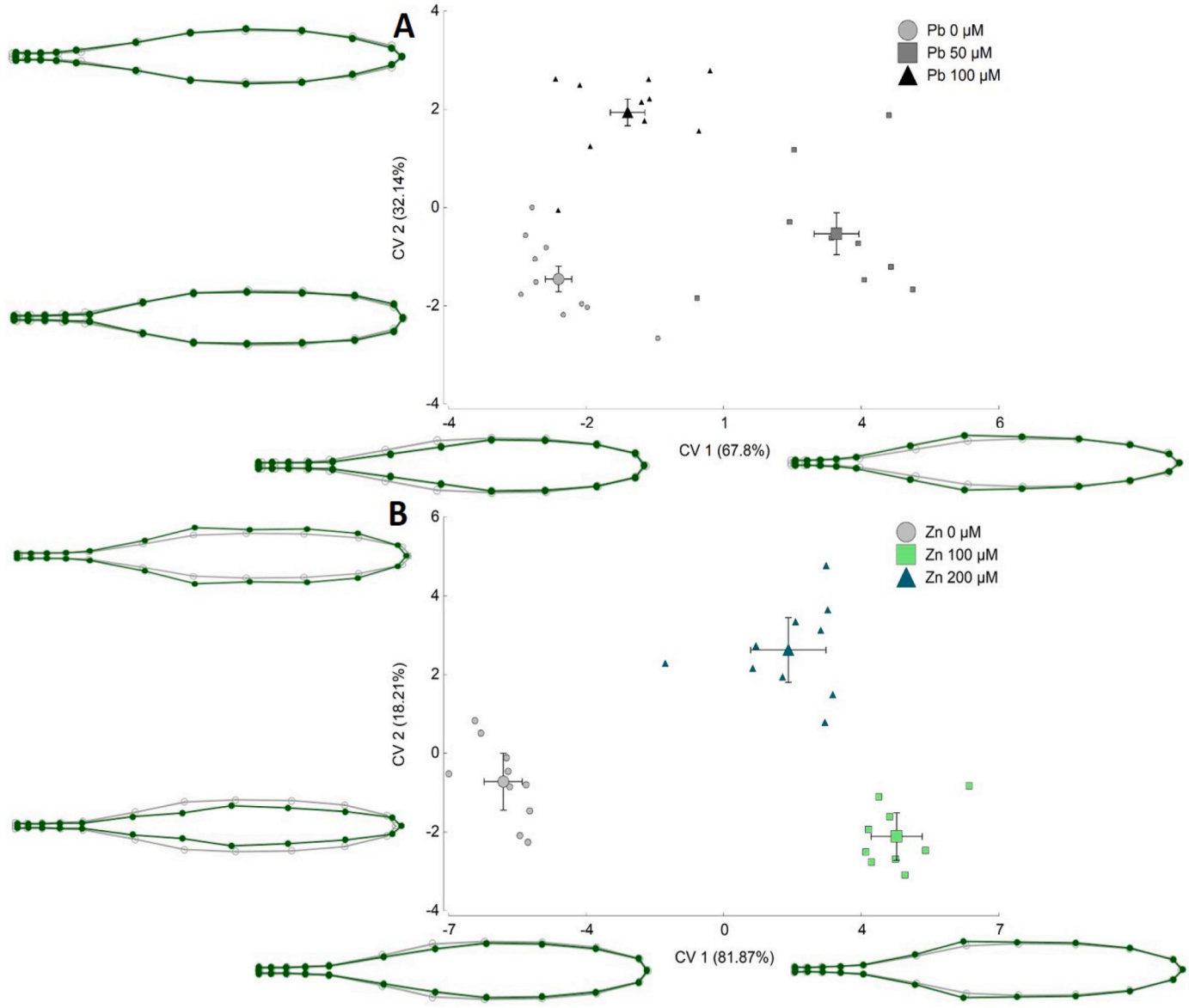

Fig. 2. Analysis of the maximum variation among (A) Pb treatments, and (B) Zn treatments in leaf shape along the first two canonical axes. The leaf graphs (wireframes) show shape changes from the positive and negative extreme shapes (green) from the consensus shape (grey) with a scale factor of ten. The percentage of variance among-treatments, relative to within-treatment variation, is presented between brackets. The biggest symbols indicate the average shapes and the whiskers the standard deviations.

3. Results

3.1. Morphometric analyses

The effect of allometry was not statistically significant ($P > 0.05$) for Pb. In contrast, it was statistically significant ($P < 0.05$) for Zn, indicating that 4.14% of the total shape variance is due to size variation. However, because this percentage was less than 5%, it was considered negligible (Zelditch et al., 2004), and subsequent analyses were done on the original shape variables for both metals.

The scatter plots of CVA showed a clear distinction among Pb and Zn treatments. The effect of Pb (Fig. 2A) was reflected along CV2, which explained 32.14% of the total variance. Positive values on this axis were associated with Pb rises and showed lanceolate leaves, whereas negative values presented spatulate shapes. On the other hand, the scatter plot of CVA for Zn (Fig. 2B) indicated a strong distinction among Zn treatments along CV1, which explained 81.87% of the total variance. Morphological changes in positive values were associated with lanceolate leaves and a slight blade expansion nearest the petiole, while opposite values showed spatulate shapes.

On the other hand, leaf size did not change between Pb treatments (ANOVA: [Pb], $P > 0.05$) but showed a significant decrease with Zn increase (ANOVA: [Zn], $P < 0.05$, Table S1).

3.2. Growth, physiological and biochemical parameters

Plants of *A. vulgatissima* survived all metal treatments and developed no visible signs of metal toxicity. In addition, shoot and root dry weights were not changed among Pb and Zn treatments (ANOVA: [Pb], $P > 0.05$, Fig. 3A; ANOVA: [Zn], $P > 0.05$, Fig. 3B). It is noteworthy that water content did not differ in Pb treatments (ANOVA: [Pb], $P > 0.05$, Fig. 3C), but it was significantly lower only in the highest amount of Zn compared to the control and 100 μM Zn treatment (ANOVA: [Zn], $P < 0.05$; Fig. 3D).

Regarding the values of Qy and ΦPSII, a reduction was observed at 50 μM Pb, while no changes were detected at 100 μM Pb. However, no statistical differences were found (ANOVA: [Pb], $P > 0.05$, Fig. 3E). In contrast, a general decrease in the values of Qy and ΦPSII was observed in all Zn treatments, but no significant differences were found between them (ANOVA: [Zn], $P > 0.05$, Fig. 3F).

An overall decrease in chlorophyll *a*, *b*, *a*+b, and carotenoids was observed for Pb-treated plants; however, no significant changes were observed in leaves across Pb addition (ANOVA: [Pb], $P > 0.05$, Fig. 4A–D). On the other hand, all pigment concentrations showed a significative reduction with increasing Zn concentrations (ANOVA: [Zn], $P < 0.05$). In 200 μM Zn-treated plants, all pigment concentrations resulted significantly lower than in control and 100 μM Zn (Fig. 4E–H). Compared to the control treatment, the reduction of chlorophyll *a*, *b*, *a*+b, and carotenoids in the 100 μM Zn treatment was between 13.32% and 13.56%, and for 200 μM Zn treatment, it was between 55.34% and 55.5%, for all pigments.

The enzyme activity in leaves of *A. vulgatissima* showed a different behavior depending on the type of enzyme and the metal treatment considered. Pb addition did not show an effect in SOD and GPx activities (ANOVA: [Pb], $P > 0.05$); Fig. 5A–B). APx activity showed a maximum at 50 μM Pb; it decreased at 100 μM Pb at the same level as the control treatment (ANOVA: [Pb], $P < 0.05$, Fig. 5C). CAT activity decreased significantly with Pb addition (ANOVA: [Pb], $P < 0.05$, Fig. 5D). On the other hand, SOD activity was significantly induced, and GPx reduced its activity with Zn increases (ANOVA: [Zn], $P < 0.05$, Fig. 5F–G). Like Pb, the middle concentration of Zn (100 μM) showed higher APx activity (ANOVA: [Zn], $P < 0.05$, Fig. 5H). Concerning CAT, no significant change was observed between the control and Zn treatments (ANOVA: [Zn], $P > 0.05$, Fig. 5I).

Metal addition produced an increment in MDA content in both metal treatments (ANOVA: [Pb], $P < 0.05$, Fig. 5E; ANOVA: [Zn], $P < 0.05$, Fig. 5J). Specifically, in the presence of Pb, the concentration of MDA increased by 15% and 28% at 50 and 100 μM, respectively. Conversely, the MDA concentration increased by 24% and 11% at 100 and 200 μM Zn, respectively.

3.3. Pb and Zn accumulation in plant tissues and indexes

Metal concentrations in *A. vulgatissima* tissues differed according to metal type, being consistently lower in control plants (ANOVA: [Pb], $P < 0.05$, Table 1; ANOVA: [Zn], $P < 0.05$, Table 1).

Pb tissue concentrations increased with Pb increases. However, it was mostly concentrated in roots, and only a little amount of Pb was translocated to shoots (Table 1). This accumulation pattern was reflected in a BCF >1 and a TF < 1 in both treatments (Table 1).

On the other hand, Zn tissue concentrations in both shoots and roots increased linearly with external Zn concentration (Table 1). Both, the BCF and TF were higher than 1 in Zn treatments, except in the control treatment, where TF was <1 (Table 1).

3.4. Integrated biological response index

Concerning Pb treatments, IBRv2 values were almost the same, 11.88 and 11.55, for 50 μM Pb and 100 μM Pb, respectively (Fig. 6A–B). When compared among Pb treatments, the concentrations of 50 μM showed induction in most of the activities of the enzymes (SOD, APx, and GPx) and intermediate levels of MDA. Conversely, the higher concentration of Pb (100 μM) resulted in elevated levels of MDA, no change in the abovementioned enzyme activities, and a greater reduction in pigments concentration and CAT activity.

Regarding Zn, the intermediate concentration of this metal (100 μM) presented the lowest IBRv2 value (8.64), which was reflected in the minor variations in the spider graph. The key biomarkers that explained this IBRv2 were SOD, APx, and MDA. In contrast, the higher concentration of Zn (200 μM) exhibited the highest value of IBRv2 (19.02), with all biomarkers, except for MDA and SOD, exhibiting significant inhibition (Fig. 6C–D).

4. Discussion

In the last decades, Pb and Zn contamination has received special attention due to its marked increase as a result of anthropogenic activities. This contamination represents a serious issue due to the persistence of these metals in the environment and can potentially harm plants, animals, and humans. In this sense, there is an increasing interest in identifying plants that can be used effectively to clean up metal contaminated environments and keep track of pollution levels. The *Atriplex* genus includes halophytic plants known for tolerating several environmental stressors, including metals, which position them as potential candidates for phytoremediation and monitoring programs. In this framework, we investigated the effect of Pb and Zn applied separately on *A. vulgatissima* and determined its accumulation capacity under experimental conditions. The findings of this study contribute to the understanding of the potential of this species for phytoremediation and monitoring of Pb and Zn pollution and highlight the importance of utilizing a battery of biomarkers and an integrative index to assess the extent of metal contamination accurately.

Even though leaf shape is genetically determined, it is likely to be subjected to selective environmental pressures, resulting in many shapes and sizes. Therefore, leaf analysis could provide valuable information about plant ecology and adaptation capacity (Nicotra et al., 2011). Morphological variations of leaf shape in *A. vulgatissima*, associated with Pb and Zn increment, displayed lanceolate leaves for both metals. However, changes in shapes for Zn were reflected along CV1, which explained an important percentage of variance (81.87%); while the Pb effect was found in CV2, explaining 32.14% of the total variance. In concordance with previous studies, the increasing metal levels in other

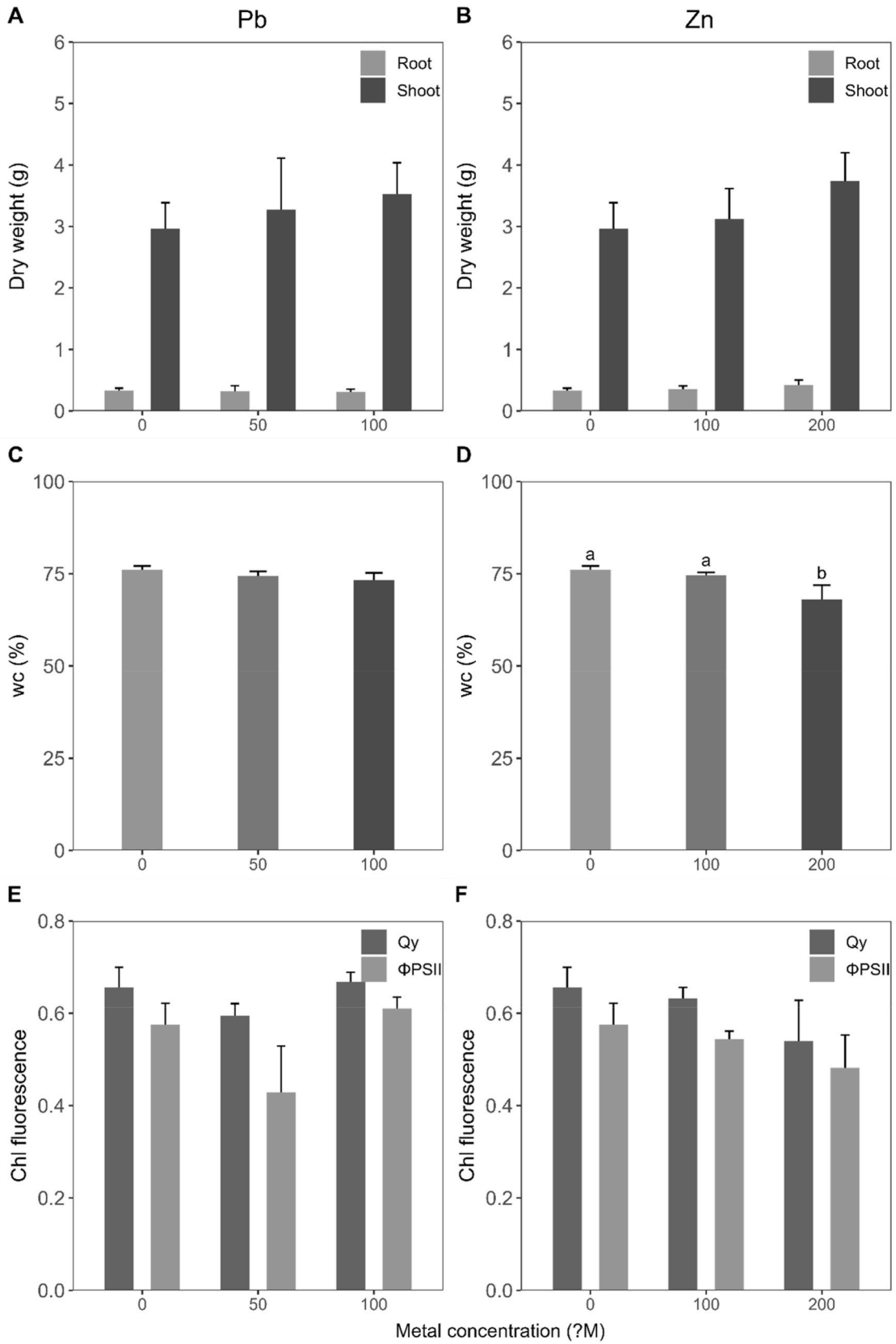

Fig. 3. (A, B) Shoot and root dry weight, (C, D) water content in leaves, (E, F) maximum quantum efficiency of PSII photochemistry (Qy) and quantum efficiency of PSII (Φ PSII) in leaves (means ± SE, n = 5) of *A.vulgatissima*. Right: Pb treatments (0, 50, and 100 μM Pb). Left: Zn treatments (0, 100 and 200 μM Zn). Different letters indicate significant differences ($P < 0.05$) among treatments in Tukey's test.

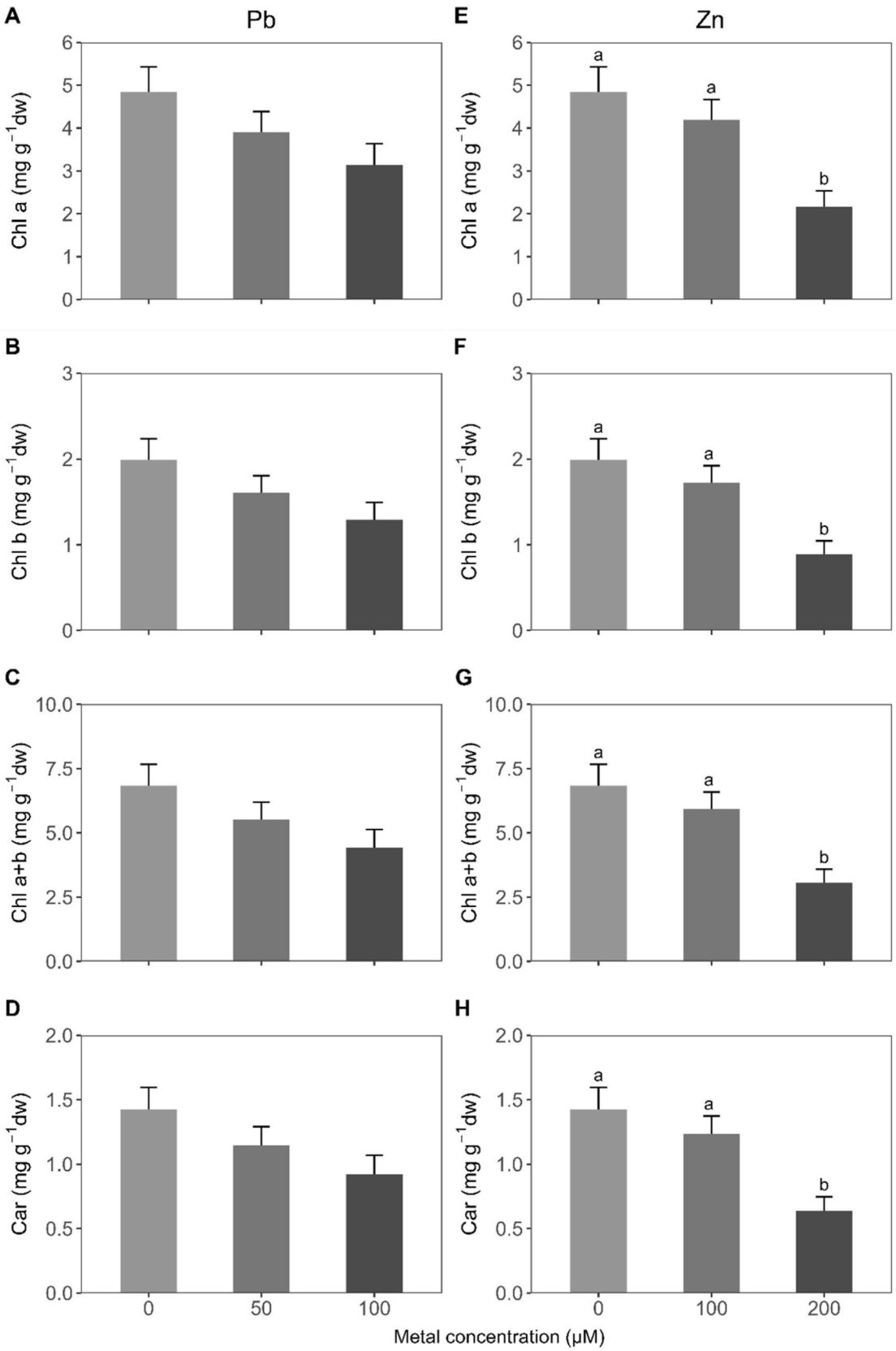

Fig. 4. Pigment concentration (means ± SE, n = 5) in leaves of *A.vulgatissima.* Right: Pb treatments (0, 50, and 100 μM Pb). Left: Zn treatments (0, 100 and 200 μM Zn). (**A**, **E**) Chlorophyll *a* (Chl a), (**B**, **F**) chlorophyll *b* (Chl b), (**C**, **G**) total chlorophyll (Chl a+b), and (**D**, **H**) carotenoids (Car). Different letters indicate significant differences ($P < 0.05$) in Tukey's test.

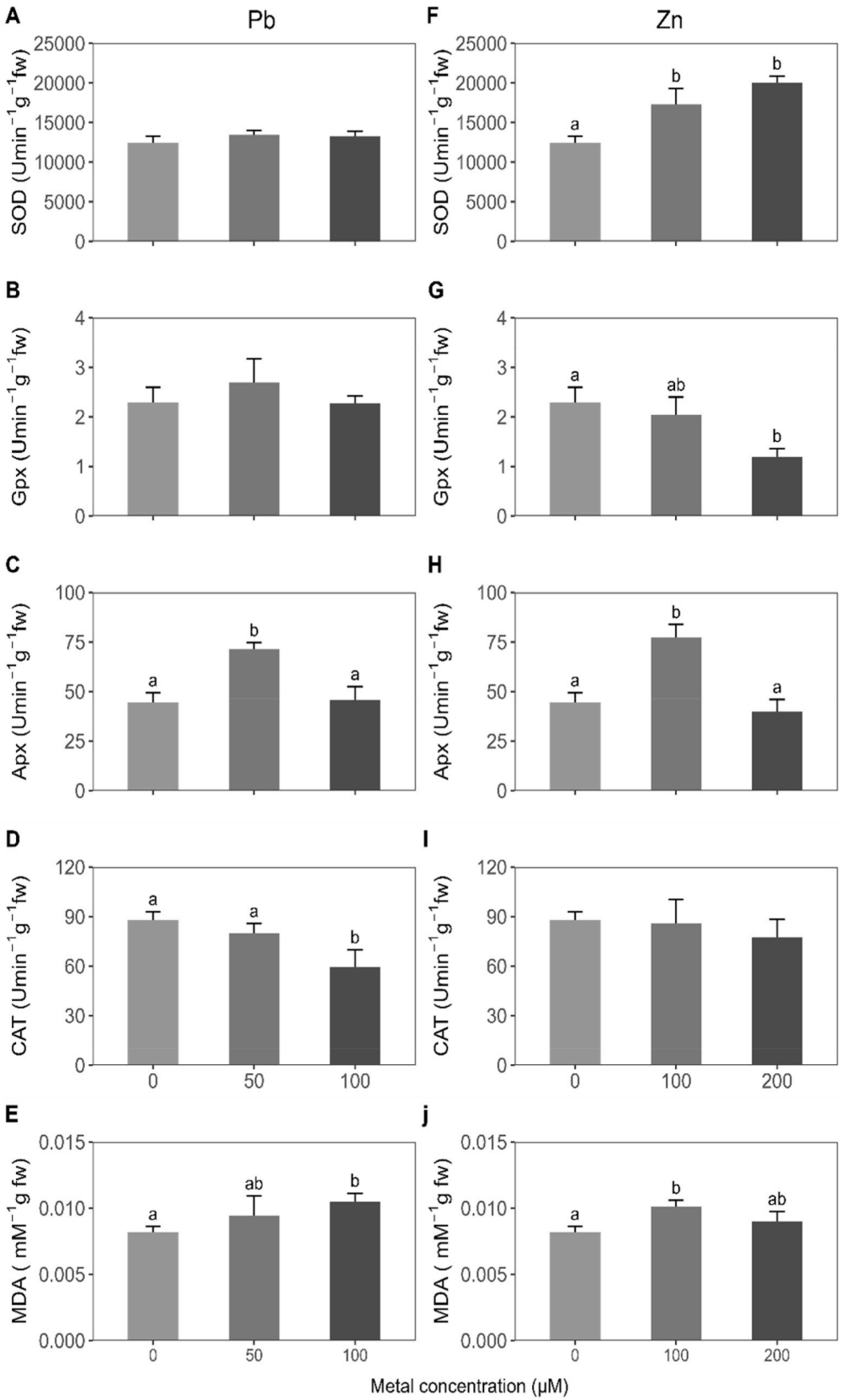

Fig. 5. Enzymatic activity (means ± SE, n = 5) in leaves of *A. vulgatissima.* Right: Pb treatments (0, 50 and 100 μM Pb). Left: Zn treatments (0, 100 and 200 μM Zn). (**A, F**) Superoxide dismutase (SOD), (**B, G**) Guaiacol peroxidase (GPx), (**C, H**) Ascorbate peroxidase (APx), (**D, I**) Catalase (CAT) and (**E, J**) Malondialdehyde (MDA). Different letters indicate significant differences ($P < 0.05$) in Tukey's test.

Table 1
Lead and Zn concentration in roots and shoots, bioaccumulation factor (BCF) and translocation factor (TF) for different treatments: 0, 50 Pb, 100 Pb, 100 Zn, and 200 Zn in *A. vulgatissima* (mean ± SE, n = 5).

Treatment (μM)		[Root] (μg g^{-1})	[Shoot] (μg g^{-1})	BCF	TF
Pb	0	9.2 ± 6.66 a	1.25 ± 0.37 a	–	0.27 ± 0.05
	50	120.7 ± 25.93 b	15.2 ± 5.19 b	11.6 ± 2.5	0.27 ± 0.09
	100	130.2 ± 18.20 b	41.0 ± 22.40 b	6.3 ± 0.88	0.28 ± 0.11
Zn	0	49.5 ± 5.94 a	26.7 ± 6.03 a	–	0.56 ± 0.11
	100	257.6 ± 20.34 b	269.5 ± 28.6 b	39.5 ± 3.11	1.1 ± 0.24
	200	327.4 ± 33.39 b	287.7 ± 17.96 b	25.1 ± 5.72	1.1 ± 0.25

halophyte plants resulted in lanceolate blades with elongated petioles (Pollicelli et al., 2018; Idaszkin et al., 2019, 2023). Furthermore, our results showed that in response to the Zn increase, the leaf exhibited prolongations of the blade in the area close to the petiole. Although the specific mechanisms behind leaf change were not addressed in this study, they could depend on the type of metal. On the other hand, the leaf size of *A. vulgatissima* was not affected by Pb increment but was reduced with the rise in Zn levels. The reduction in leaf size at 200 μM Zn was possibly due to the loss of turgidity resulting from low water content in leaves, which consequently inhibited cell expansion (Kaur and Garg, 2021). This finding is consistent with several studies that have reported a reduction in leaf size or other plant structures, such as sepals, petals, and stamens, in response to different pollutants (Syed et al., 2008; Veličković, 2010; Vujić et al., 2015a, 2015b).

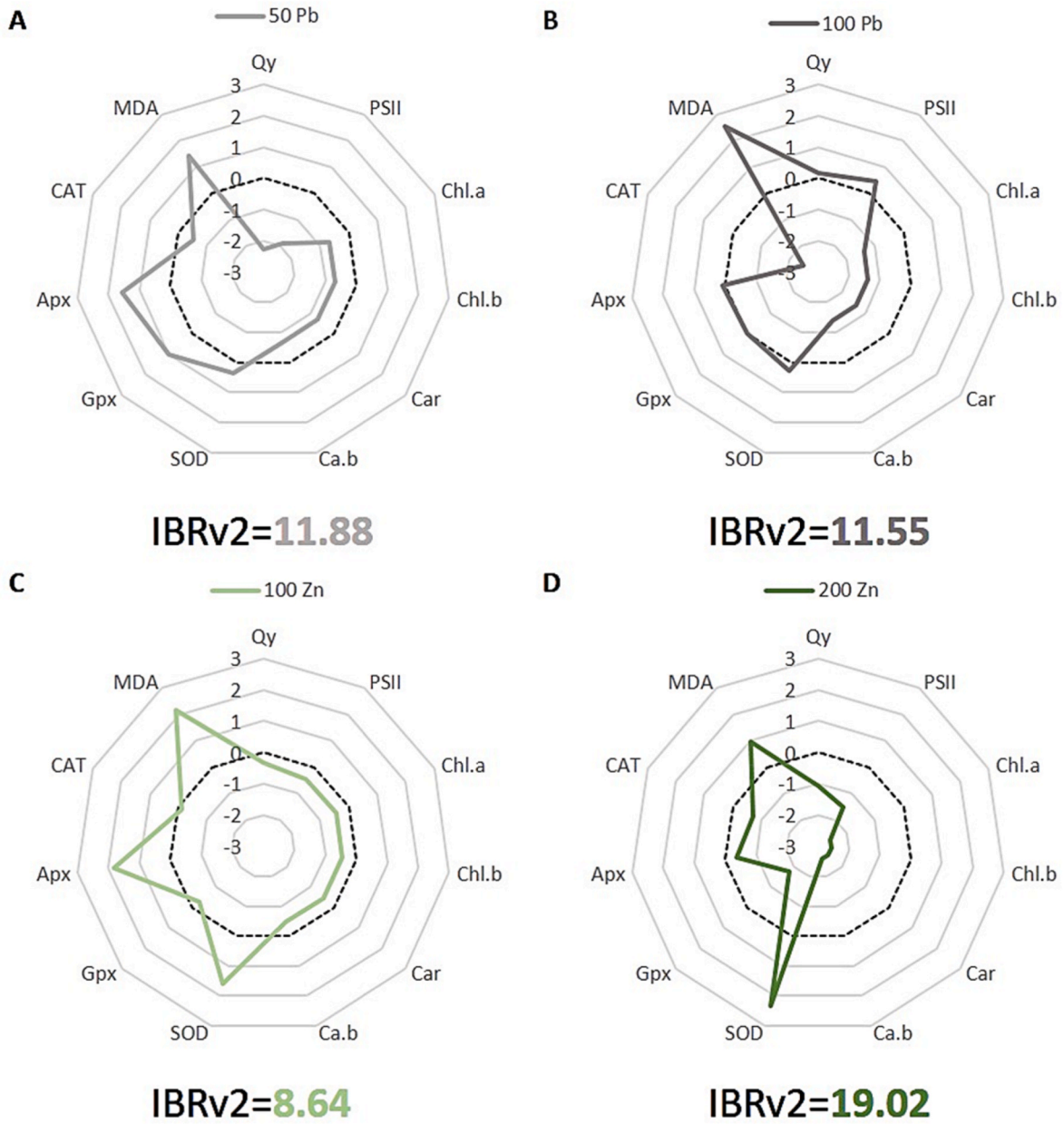

Fig. 6. Spider graphs of Integrated Biological Response version 2 (IBRv2) based on the following biomarkers: Quantum yield (Qy), the quantum efficiency of photosystem II (PSII), chlorophyll *a* (Chl a), chlorophyll *b* (Chl b), carotenoids (Car), total chlorophyll content (Chl a.b), superoxide dismutase (SOD), guaiacol peroxidase (GPx), ascorbate peroxidase (APx), catalase (CAT), and malondialdehyde (MDA) in leaves of *Atriplex vulgatissima*. Black dotted lines correspond to reference levels (control treatment), and color lines reflect the IBRv2 index from each treatment: (**A**) 50 Pb, (**B**) 100 Pb, (**C**) 100 Zn, and (**D**) 200 Zn. Values above control reflect induction, while below control indicate inhibition of the biomarker.

The metal concentrations in *A. vulgatissima* were between phytotoxic levels for general plants, 30–300 μg g^{-1} for Pb, and 100–500 μg g^{-1} for Zn (Kabata-Pendias, 2011). However, no visible damage was observed in plants treated with these metals. In addition, all plants produced similar shoot and root dry weights under different metal treatments. Similar results were found when *Atriplex halimus* L. was subjected to 800 μM Pb (Manousaki and Kalogerakis, 2009) and when exposed to a range of Pb concentration (from 0 to 600 μM) (Bankaji et al., 2019). Nevertheless, it has been documented that Pb contamination impairs plant growth (Zulfiqar et al., 2019). On the other hand, Zhao et al. (2000) found that shoot and root dry weights were unaffected due to the Zn increase (1–1000 μM Zn) in the hyperaccumulator *Arabidopsis halleri*. Like Pb, different studies have demonstrated a decline in growth parameters of diverse plant crops due to Zn increment plants (Paradisone et al., 2015; Rouphael et al., 2016; Aghajanzadeh et al., 2020).

Metal toxicity decreases relative water content (Kabata-Pendias, 2011). In our study, while the water content of *A. vulgatissima* remained unaffected by the increment of Pb, it decreased significantly with the higher Zn levels. This result agrees with other parameters measuring at 200 μM Zn, which indicates a certain grade of stress due to the accumulation of Zn in shoots. Maintaining water status accountable for balanced water potential, despite metal addition, could be a strategy for improving the tolerance of halophyte plants (Singh et al., 2023).

Chlorophyll fluorescence parameters are used to estimate plants' capacity to perform photosynthesis, which is highly metal sensitive (Maxwell and Johnson, 2000). However, we did not find an effect on PSII and Qy due to increased Pb and Zn concentrations. Even though several studies in plants have found that these metals affect the photosynthetic parameters (Mateos-Naranjo et al., 2008; Mateos-Naranjo et al., 2018; Huang et al., 2019), there exists evidence that the integrity and functionality of the photosynthesis apparatus were unaffected at a concentration of 100 mM Zn, in the halophytic species *Juncus acutus* (Mateos-Naranjo et al., 2014). Moreover, it is widely acknowledged that metals produce changes in chloroplast structure and reductions of photosynthetic pigments (Aggarwal et al., 2012; Rai et al., 2016). Comparing the effect of Pb and Zn increment on photosynthetic pigment concentrations in *A. vulgatissima*, we found that they decreased only in plants at the highest Zn concentration. This is probably because Zn is a highly mobile element within plants and is more easily transported to leaves than Pb, which agrees with the metal concentrations detected and reflected in the TF values. However, a study in *A. halimus* showed that chlorophyll content decreased under Pb increment (at 600 μM Pb) but did not change in Zn treatments (between 200 and 600 μM Zn) (Bankaji et al., 2019). Thus, the effect of the different types of metals on the photosynthetic apparatus could be a species-specific response.

The metal tolerance of halophytes is strongly linked with an effective antioxidant system, which acts synergistically to scavenge ROS and improve or alleviate stressful conditions and their damaging effect (Kumari et al., 2019). It is known that SOD is the first defense against ROS, which sequesters O^{2-} (superoxide ions), destroys them, and forms less harmful O_2 and hydrogen peroxide (H_2O_2) molecules. SOD activity did not show differences in Pb treatments but increased according to Zn rises. The increment in SOD activity may be attributed to an enhancement of ROS due to Zn accumulation in leaves, which can affect the structure of the thylakoid membrane in chloroplasts and the Chl activation due to the replacement of Mg^{+2} by Zn^{+2} at the sites of water photolysis, producing an increment in ROS (Kaur and Garg, 2021). Consequently, high levels of SOD could result in an advantage that allows plants to resist oxidative damage and maintain the overall defense system. Studies conducted on species of *Lolium perenne* and *Triticum aestivum* L. have also reported enhanced SOD in leaves under different Zn treatments (Bonnet et al., 2000; Kanwal et al., 2016). On the other hand, CAT is an enzyme that scavenges H_2O_2 by degrading it into H_2O and O_2. CAT activity showed a significant decline at the highest Pb treatment. This reduction can be attributed to Pb ions interference in enzyme synthesis or assembly of enzyme subunits or its degradation due to levels of ROS (Rascio and Nevari-Izzo, 2011). Rastgoo and Alemzadeh (2011) described the same pattern of CAT activity in *Aeluropus littoralis* treated with various doses of Pb. However, a study with rice exposed to similar Pb concentrations indicated that CAT was not changed in a short period, but its activity decreased after 96 h of treatments (Thakur et al., 2017). APx and GPx also play an important role in detoxifying the H_2O_2. In this study, Apx showed a hormesis phenomenon, *i.e.*, a stimulatory effect under intermediate Pb and Zn concentration, whereas, at higher levels of these metals, its activity was similar to the control (Calabrese et al., 2007). In addition, GPx activity did not show different activity under Pb treatments, whereas Zn increment in the medium inhibited GPx activity, probably due to its inactivation by H_2O_2 accumulation. This same pattern of GPx activity was described for the halophyte *Atriplex haliums* under Zn increment (Bankaji et al., 2019). It is known that both deficiency and excess of metals can inhibit or stimulate enzyme activity depending on several factors, including plant species, metal type and its doses, and time of exposure (Zulfiqar et al., 2019; Kaur and Garg, 2021).

Regarding MDA content, its increment in response to Pb and Zn exposure indicates damage in biological membranes and induction of oxidative stress, which might result from the fact that the detoxification mechanism was insufficient (Sharma and Dubey, 2005; Kaur and Garg, 2021). The decline, deficiency, or alteration in antioxidant enzymatic activity could increase ROS and ultimately alter membrane integrity (Devi and Prasad, 1999). In agreement, many studies have reported membrane damage in different tissues of plants in response to Pb or Zn stress (Dey et al., 2007; Kaur et al., 2015; Ashraf et al., 2017; Thakur et al., 2017; Kaur and Garg, 2021).

Our results showed that metal concentrations in shoots and roots differed among the different metal treatments. The accumulation patterns of both metals exceeded the essential requirement for roots and shoots (<1 μg $g^{-.1}$ for Pb and 50 μg g^{-1} for Zn) and reached toxicity levels in aboveground tissues (between 0.6 and 28 μg $g^{-.1}$ for Pb and 100–300 μg g^{-1} for Zn), indicating above normal metal concentrations and showing high plant resistance (Krämer et al., 2010; Aziz and Mujeeb, 2022). Pb was accumulated mainly in the roots, with only a tiny amount translocating to the shoots. Pb was probably detoxified by complexation with organic acids or amino acids, binding to peptides, and/or sequestered into vacuoles, allowing only free ions to be transported to shoot (Rascio and Navari-Izzo, 2011). Moreover, these results suggest that Pb was restricted to apoplastic space and that some barriers, such as endodermal Casparian strips, may stop or prevent translocation from the roots to the shoots. In agreement with our findings, the halophyte *Limonium brasiliense* exposed to a similar range of Pb in experimental conditions showed similar behavior of these metals within plants (Idaszkin et al., 2019, 2023). Several studies on wild plant species growing in soils contaminated by metals have reported similar patterns of accumulation in belowground tissues (Brunetti et al., 2009; Midhat et al., 2019). Since Pb BCF was higher than one and TF was less than one, *A. vulgatissima* could function as a phytoestabilizator of this metal (Anjum et al., 2014). On the other hand, Zn was readily translocated to leaves. For this metal, BCF was much higher than one, and TF exceeded unity for both Zn doses. Although *A. vulgatissima* did not reach shoot accumulation levels of Zn 3000 μg $g^{-}1$ required to be considered a hyperaccumulator, as suggested by Van der Ent et al. (2013), it could be considered a phytoextractor due to its efficiency of Zn accumulation in the shoot. Many species of the Amaranthaceae family have displayed trends towards accumulating high levels of Zn in both roots and shoots (BCF and TF both higher than one), suggesting active accumulation of this metal (Alam et al., 2021). A TF above the unit suggests that the uptake occurs via active transporters across root plasmalemma. This energy expenditure could produce an energetic demand that, in the long term, produces an unbalance of homeostasis, which could explain the stress observed at the Zn treatment 200 μM. The observed differences in TF between studied metals can be explained by the low mobility of Pb within the plant compared with the high mobility that Zn owns. Mujeeb

et al. (2021) reported similar Pb and Zn accumulation patterns in *Atriplex stocksii* in polluted Karachi Coast (Pakistan) soils to those we observed in *A. vulgatissima*.

In the study of the impact of metals on plants, more than a single biomarker is required to determine the extent of the environmental impact. Thus, using a battery of biomarkers based on complementary parameters is essential to accurately assess the effects of metals on plants. Moreover, integrating this biomarker information into an integrative index is crucial for providing a complete diagnosis of environmental pollutants. To achieve this, we selected eleven biomarkers to separately evaluate the toxicity of Pb and Zn using the IBRv2 index. Although a previous study has used IBR to assess salt marsh plants' health status (Duarte et al., 2018), our study is the first to utilize the IBRv2 index (Sanchez et al., 2013), which not only removes the dependency on the arrangement of biomarkers on the start plot but also allows us to discriminate induction and inhibition for each biomarker. The investigated biomarkers were induced or inhibited according to different metal treatments. Among treatments, the Zn treatments showed higher and lower IBRv2 for 100 and 200 μM Zn, respectively. As expected, the IBRv2 showed a higher value for Pb treatment at the same Pb and Zn concentration, indicating that plants were more affected by Pb despite its lower shoot transport. All tested biomarkers resulted in sensitive tools and were appropriated to test Pb and Zn toxicity in *A. vulgatissima* when those metals occur in isolation; however, future research should focus on the synergic effect when Pb and Zn rise simultaneously in the environment.

5. Conclusion

This study highlights the remarkable ability of *A. vulgatissima* to survive and adapt the leaf shape to high levels of Pb and Zn, as well as their ability to regulate photosynthetic activity under different environmental conditions without showing any visible signs of toxicity. *A. vulgatissima* could be a suitable candidate to phytoestabilize Pb and phytoextract Zn, allowing minimizing Pb migration and removing Zn from the salt marsh environment. Pb and Zn had no significant impact on biomass and photosynthetic parameters. Antioxidant enzyme activity was different according to type and metal concentrations. However, signals such as increased MDA levels would let glimpses of stress at the highest Pb and Zn concentration. Besides, Zn 200 μM treatment was the most affected in several measured biomarkers. The IBRv2 is a simple tool to differentiate and evaluate the Pb and Zn effects on plants' health status.

Future studies could account for the mixture of Pb and Zn to cover possible interaction effects between these metals and the screening in field conditions. Understanding the capacity of native species to cope with metals and describe accumulation patterns could produce a better phytoremediation strategy and management of contaminated areas.

Author contributions

Authors' individual contributions María de la Paz Pollicelli: Writing –original draft, review & editing, Conceptualization, Investigation, Formal analysis. Federico Márquez: Writing – review & editing, Conceptualization, Investigation, Formal analysis, Funding acquisition. María Débora Pollicelli: Writing – review, Formal analysis. Yanina L. Idaszkin: Writing – review & editing, Conceptualization, Investigation, Formal analysis, Funding acquisition.

Declaration of competing interest

The authors declare that they have no known competing financial interests or personal relationships that could have appeared to influence the work reported in this paper.

Data availability

Data will be made available on request.

Acknowledgements

The authors would like to thank Tomas Bosco for his assistance in laboratory work and Julio Rua for their collaboration in field activities. We are especially grateful to ALUAR Aluminio Argentino S.A.I.C. who provided us with liquid N_2, given that it is essential at the end of the experiment. This study was supported by the Fondo para la Investigación Científica y Tecnológica (PICTs Nº 2016-0017 and Nº 2018–03802) and Neotropical Grassland Conservancy (Derald G. Langham Memorial Research Grant). This investigation is part of MPP's PhD thesis in the University Nacional de la Patagonia San Juan Bosco for which the Consejo Nacional de Investigaciones Científicas y Técnicas (CONICET, Argentina) has granted her a postgraduate fellowship.

Appendix A. Supplementary data

Supplementary data to this article can be found online at https://doi.org/10.1016/j.chemosphere.2023.140110.

References

Aggarwal, A., Sharma, I., Tripathi, B.N., Munjal, A.K., Baunthiyal, M., Sharma, V., 2012. Metal Toxicity and Photosynthesis. Photosynthesis: Overviews on Recent Progress and Future Perspectives, pp. 229–236.

Aghajanzadeh, T.A., Prajapati, D.H., Burow, M., 2020. Differential partitioning of thiols and glucosinolates between shoot and root in Chinese cabbage upon excess zinc exposure. J. Plant Physiol. 244, 153088.

Alam, M.R., Islam, R., Tran, T.K.A., LeVan, D., Rahman, M.M., Griffin, A.S., Richard, M. K.Y., MacFarlane, G.R., 2021. Global patterns of accumulation and partitioning of metals in halophytic saltmarsh taxa: a phylogenetic comparative approach. J. Hazard Mater. 414, 125515.

Alam, M.R., Rahman, M.M., Yu, R.M.K., MacFarlane, G.R., 2023. Offspring of metal contaminated saltmarsh (*Juncus acutus*) exhibit tolerance to the essential metal Zn but not the nonessential metal Pb. Environ. Pollut. 121333.

Ali, H., Khan, E., Sajad, M.A., 2013. Phytoremediation of heavy metals—concepts and applications. Chemosphere 91 (7), 869–881.

Anjum, N.A., Ahmad, I., Valega, M., Mohmood, I., Gill, S.S., Tuteja, N., Pereira, E., 2014. Salt marsh halophyte services to metal–metalloid remediation: assessment of the processes and underlying mechanisms. Crit. Rev. Environ. Sci. Technol. 44 (18), 2038–2106.

Ashraf, U., Hussain, S., Anjum, S.A., Abbas, F., Tanveer, M., Noor, M.A., Tang, X., 2017. Alterations in growth, oxidative damage, and metal uptake of five aromatic rice cultivars under lead toxicity. Plant Physiol. Biochem. 115, 461–471.

Aziz, I., Mujeeb, A., 2022. Halophytes for phytoremediation of hazardous metal (loid) s: a terse review on metal tolerance, bio-indication and hyperaccumulation. J. Hazard Mater. 424, 127309.

Balafrej, H., Bogusz, D., Triqui, Z.E.A., Guedira, A., Bendaou, N., Smouni, A., Fahr, M., 2020. Zinc hyperaccumulation in plants: a review. Plants 9 (5), 562.

Bankaji, I., Pérez-Clemente, R.M., Caçador, I., Sleimi, N., 2019. Accumulation potential of *Atriplex halimus* to zinc and lead combined with NaCl: effects on physiological parameters and antioxidant enzymes activities. S. Afr. J. Bot. 123, 51–61.

Beliaeff, B., Burgeot, T., 2002. Integrated biomarker response: a useful tool for ecological risk assessment. Environ. Toxicol. Chem.: Int. J. 21 (6), 1316–1322.

Bergmeyer, H.U., Gawehn, K., Grassl, M., 1974. Enzymes as biochemical reagents. In: Bergmeyer, H.U. (Ed.), Methods in Enzymatic Analysis. Academic Press, New York, pp. 425–556.

Bonnet, M., Camares, O., Veisseire, P., 2000. Effects of zinc and influence of *Acremonium lolii* on growth parameters, chlorophyll a fluorescence and antioxidant enzyme activities of ryegrass (*Lolium perenne* L. cv Apollo). J. Exp. Bot. 51 (346), 945–953.

Brignone, N.F., Denham, S.S., Pozner, R., 2016. Synopsis of the genus *Atriplex* (Amaranthaceae, chenopodioideae) for south America. Aust. Sys. Bot. 29 (5), 324–357.

Brunetti, G., Soler-Rovira, P., Farrag, K., Senesi, N., 2009. Tolerance and accumulation of heavy metals by wild plant species grown in contaminated soils in Apulia region. Southern Italy. Plant Soil 318, 285–298.

Calabrese, E.J., Bachmann, K.A., Bailer, A.J., Bolger, P.M., Borak, J., Cai, L., Mattso, M. P., 2007. Biological stress response terminology: integrating the concepts of adaptive response and preconditioning stress within a hormetic dose–response framework. Toxicol. Appl. Pharmacol. 222 (1), 122–128.

Čalasan, A.Ž., Hammen, S., Sukhorukov, A.P., McDonald, J.T., Brignone, N.F., Böhnert, T., Kadereit, G., 2022. From continental Asia into the world: global historical biogeography of the saltbush genus *Atriplex* (Chenopodieae, Chenopodioideae, Amaranthaceae). Perspect. Plant Ecol. Evol. Syst. 54, 125660.

Caparrós, P.G., Ozturk, M., Gul, A., Batool, T.S., Pirasteh-Anosheh, H., Unal, B.T., Altay, V., Toderich, K.N., 2022. Halophytes have potential as heavy metal phytoremediators: a comprehensive review. Environ. Exp. Bot. 193, 104666.
Devi, S.R., Prasad, M.N.V., 1999. Membrane lipid alterations in heavy metal exposed plants. In: Heavy Metal Stress in Plants. Springer, Berlin, Heidelberg, pp. 99–116.
Dey, S.K., Dey, J., Patra, S., Pothal, D., 2007. Changes in the antioxidative enzyme activities and lipid peroxidation in wheat seedlings exposed to cadmium and lead stress. Braz. J. Plant Physiol. 19, 53–60.
Dresler, S., Wójciak-Kosior, M., Sowa, I., Stanisławski, G., Bany, I., Wójcik, M., 2017. Effect of short-term Zn/Pb or long-term multi-metal stress on physiological and morphological parameters of metallicolous and nonmetallicolous *Echium vulgare* L. populations. Plant Physiol. Biochem. 115, 380–389.
Dryden, I., Mardia, K., 1998. Statistical Shape Analysis. John Wiley y Sons, Chichester, UK.
Duarte, B., Carreiras, J., Pérez-Romero, J.A., Mateos-Naranjo, E., Redondo-Gomez, S., Matos, A.R., Cacador, I., 2018. Halophyte fatty acids as biomarkers of anthropogenic-driven contamination in Mediterranean marshes: sentinel species survey and development of an integrated biomarker response (IBR) index. Ecol. Indic. 87, 86–96.
Grigore, M.N., Toma, C., 2021. Morphological and anatomical adaptations of halophytes: a review. Handbook of Halophytes: From Molecules to Ecosystems towards Biosaline Agriculture 1079–1221.
Gunz, P., Mitteroecker, P., Bookstein, F.L., 2005. Semilandmarks in three dimensions. In: Slice, D.E. (Ed.), Modern Morphometrics in Physical Anthropology. Springer, Boston, pp. 73–98.
Hasnaoui, S.E., Fahr, M., Keller, C., Levard, C., Angeletti, B., Chaurand, P., Smouni, A., 2020. Screening of native plants growing on a Pb/Zn mining area in eastern Morocco: perspectives for phytoremediation. Plants 9 (11), 1458.
Heath, R.L., Packer, L., 1968. Photoperoxidation in isolated chloroplasts: I. Kinetics and stoichiometry of fatty acid peroxidation. Arch. Biochem. Biophys. 125 (1), 189–198.
Huang, X.H., Zhu, F., Yan, W.D., Chen, X.Y., Wang, G.J., Wang, R.J., 2019. Effects of Pb and Zn toxicity on chlorophyll fluorescence and biomass production of *Koelreuteria paniculata* and *Zelkova schneideriana* young plants. Photosynthetica 57 (2), 688–697.
Idaszkin, Y.L., Márquez, F., Mateos-Naranjo, E., Pollicelli, M.P., Cisneros, H.S., 2019. Multidimensional approach to evaluate *Limonium brasiliense* as source of early biomarkers for lead pollution monitoring under different saline conditions. Ecol. Indic. 104, 567–575.
Idaszkin, Y.L., Pollicelli, M.P., Márquez, F., 2023. Assessment of halophyte plant phenotypic responses under heavy metals pollution. Implications for monitoring and phytoremediation. Environ. Pollut. 331, 121916.
Jin, X., Shi, C., Yu, C.Y., Yamada, T., Sacks, E.J., 2017. Determination of leaf water content by visible and near-infrared spectrometry and multivariate calibration in *Miscanthus*. Front. Plant Sci. 8, 721.
Kabata-Pendias, A., 2011. Trace Elements in Soils and Plants. CRC Press, fourth ed. Taylor & Francis Group, LLC, USA, p. 534.
Kachout, S.S., Ennajah, A., Guenni, K., Ghorbel, N., Zoghlami, A., 2023. Potential of halophytic plant *Atriplex hortensis* for phytoremediation of metal-contaminated soils in the mine of Tamra. Soil Sediment Contam. An International Journal 1–16.
Kachout, S.S., Mansoura, A.B., Leclerc, J.C., Mechergui, R., Rejeb, M.N., Ouerghi, Z., 2010. Effects of heavy metals on antioxidant activities of: *Atriplex hortensis* and A. rosea. Elec. J. Env. Agricult. Food Chem. 9 (3).
Kanwal, S., Bano, A., Malik, R.N., 2016. Role of arbuscular mycorrhizal fungi in phytoremediation of heavy metals and efects on growth and biochemical activities of wheat (*Triticum aestivum* L.) plants in Zn contaminated soils. Afr. J. Biotechnol. 15 (20), 872–883.
Kaur, G., Singh, H.P., Batish, D.R., Kohli, R.K., 2015. Adaptations to oxidative stress in *Zea mays* roots under short-term Pb 2+ exposure. Biologia 70, 190–197.
Kaur, H., Garg, N., 2021. Zinc toxicity in plants: a review. Planta 253 (6), 129.
Klingenberg, C.P., 2011. MorphoJ: an integrated software package for geometric morphometrics. Molec. Ecol. Resour. 11 (2), 353–357.
Klingenberg, C.P., Barluenga, M., Meyer, A., 2002. Shape analysis of symmetric structures: quantifying variation among individuals and asymmetry. Evolution 56, 1909–1920.
Krämer, U., 2010. Metal hyperaccumulation in plants. Annu. Rev. Plant Biol. 61, 517–534.
Kumari, A., Sheokand, S., Kumar, A., Mann, A., Kumar, N., Devi, S., Meena, B.L., 2019. Halophyte growth and physiology under metal toxicity. Ecophysiology, Abiotic Stress Responses and Utilization of Halophytes 83–113.
Laghlimi, M., Elouadihi, N., Baghdad, B., Moussade, R., Laghrour, M., Bouabdli, A., 2022. Influence of compost and chemical fertilizer on multi-metal contaminated mine tailings phytostabilization by *Atriplex nummularia*. Ecol. Eng. Environ. Technol. 23 (6), 204–215.
Lichtenthaler, H.K., 1987. Chlorophylls and carotenoids: pigments of photosynthetic biomembranes. In: Methods in Enzymology, vol. 148. Academic Press, pp. 350–382.
Lomartire, S., Marques, J.C., Gonçalve, A.M., 2021. Biomarkers based tools to assess environmental and chemical stressors in aquatic systems. Ecol. Indic. 122, 107207.
Manousaki, E., Kalogerakis, N., 2009. Phytoextraction of Pb and Cd by the Mediterranean saltbush (*Atriplex halimus* L.): metal uptake in relation to salinity. Environ. Sci. Pollut. Res. 16, 844–854.
Manousaki, E., Kalogerakis, N., 2011. Halophytes present new opportunities in phytoremediation of heavy metals and saline soils. Ind. Eng. Chem. Res. 50 (2), 656–660.
Marklund, S., Marklund, G., 1974. Involvement of the superoxide anion radical in the autoxidation of pyrogallol and a convenient assay for superoxide dismutase. Eur. J. Biochem. 47 (3), 469–474.
Mateos-Naranjo, E., Castellanos, E.M., Perez-Martin, A., 2014. Zinc tolerance and accumulation in the halophytic species *Juncus acutus*. Env. Exp. Bot. 100, 114–121.
Mateos-Naranjo, E., Pérez-Romero, J.A., Redondo-Gómez, S., Mesa-Marín, J., Castellanos, E.M., Davy, A.J., 2018. Salinity alleviates zinc toxicity in the saltmarsh zinc-accumulator *Juncus acutus*. Ecotoxicol. Environ. Saf. 163, 478–485.
Mateos-Naranjo, E., Redondo-Gómez, S., Cambrollé, J., Luque, T., Figueroa, M.E., 2008. Growth and photosynthetic responses to zinc stress of an invasive cordgrass, *Spartina densiflora*. Plant Biol 10 (6), 754–762.
Maxwell, K., Johnson, G.N., 2000. Chlorophyll fluorescence-a practical guide. J. Exp. Bot. 51 (345), 659–668.
Mesnoua, M., Mateos-Naranjo, E., Barcia-Piedras, J.M., Pérez-Romero, J.A., Lotmani, B., Redondo-Gómez, S., 2016. Physiological and biochemical mechanisms preventing Cd-toxicity in the hyperaccumulator *Atriplex halimus* L. Plant Physiol. Biochem. 106, 30–38.
Midhat, L., Ouazzani, N., Hejjaj, A., Ouhammou, A., Mandi, L., 2019. Accumulation of heavy metals in metallophytes from three mining sites (Southern Centre Morocco) and evaluation of their phytoremediation potential. Ecotoxicol. Environ. Saf. 169, 150–160.
Milinkovitch, T., Geffard, O., Geffard, A., Mouneyrac, C., Chaumot, A., Xuereb, B., Sanchez, W., 2019. Biomarkers as tools for monitoring within the Water Framework Directive context: concept, opinions and advancement of expertise. Environ. Sci. Pollut. Res. 26, 32759–32763.
Mujeeb, A., Aziz, I., Ahmed, M.Z., Shafiq, S., Fatima, S., Alvi, SKk, 2021. Spatial and seasonal metal variation, bioaccumulation and biomonitoring potential of halophytes from littoral zones of the Karachi. Coast. Sci. Total Environ. 781, 146715.
Nicotra, A.B., Leigh, A., Boyce, C.K., Jones, C.S., Niklas, K.J., Royer, D.L., Tsukaya, H., 2011. The evolution and functional significance of leaf shape in the angiosperms. Funct. Plant Biol. 38 (7), 535–552.
Paradisone, V., Barrameda-Medina, Y., Montesinos-Pereira, D., Romer, L., Esposito, S., Ruiz, J.M., 2015. Roles of some nitrogenous compounds protectors in the resistance to zinc toxicity in *Lactuca sativa* cv. Phillips and *Brassica oleracea* cv. Bronco. Acta Physiol Plant 37, 137.
Pérez-Romero, J.A., Idaszkin, Y.L., Duarte, B., Baeta, A., Marques, J.C., Redondo-Gómez, S., Caçador, I., Mateos-Naranjo, E., 2018. Atmospheric CO2 enrichment effect on the Cu-tolerance of the C4 cordgrass *Spartina densiflora*. J. Plant Physiol. 220, 155–166.
Pinheiro, J.C., Bates, D.M., 2006. Mixed-effects Models in S and S-PLUS. Springer science and business media.
Pollicelli, M.P., Idaszkin, Y.L., Gonzalez-José, R., Márquez, F., 2018. Leaf shape variation as a potential biomarker of soil pollution. Ecotoxicol. Environ. Saf. 164, 69–74.
Rai, R., Agrawal, M., Agrawal, S.B., 2016. Impact of heavy metals on physiological processes of plants: with special reference to photosynthetic system. In: Singh, A., Prasad, S.M., Singh, R.P (Eds.), Plant responses to xenobiotics. Springer, Singapore, pp. 127–140.
Rascio, N., Navari-Izzo, F., 2011. Heavy metal hyperaccumulating plants: how and why do they do it? And what makes them so interesting? Plant sci 180 (2), 169–181.
Rastgoo, L., Alemzadeh, A., 2011. Biochemical responses of Gouan (*'Aeluropus littoralis'*) to heavy metals stress. Aust. J. Crop. Sci. 5 (4), 375–383.
Resende, A.C., Pereira, D.M.C., Resende, M.A.C., 2022. Package 'IBRtools'.
Roe, R.A., Yu, R.M.K., Rahman, M.M., MacFarlane, G.R., 2021. Towards adverse outcome pathways for metals in saltmarsh ecosystems–A review. J. Hazard Mater. 416, 126252.
Rohlf, F.J., 2017a. A TPSDig2. Department of Ecology and Evolution, State University of New York, Stony Brook, New York, Version 2.3.
Rohlf, F.J., 2017b. b TPSUtil, Version 1.74. Department of Ecology and Evolution, State University of New York, Stony Brook, New York.
Rohlf, F.J., 2017c. TPSRelw v.1.67. Department of Ecology and Evolution, State University of New York, Stony Brook, New York.
Rouphael, Y., Colla, G., Bernardo, L., Kane, D., Trevisan, M., Lucini, L., 2016. Zinc excess triggered polyamines accumulation in lettuce root metabolome, as compared to osmotic stress under high salinity. Front. Plant Sci. 7, 842.
Sanchez, W., Burgeot, T., Porcher, J.M., 2013. A novel "Integrated Biomarker Response" calculation based on reference deviation concept. Environ. Sci. Pollut. Res. 20, 2721–2725.
Saxena, G., Purchase, D., Mulla, S.I., Saratale, G.D., Bharagava, R.N., 2020. Phytoremediation of heavy metal-contaminated sites: eco-environmental concerns, field studies, sustainability issues, and future prospects. Rev. Environ. Contam. Toxicol. 249, 71–131.
Sharma, P., Dubey, R.S., 2005. Lead toxicity in plants. Braz. J. Plant Physiol. 17, 35–52.
Shen, X., Dai, M., Yang, J., Sun, L., Tan, X., Peng, C., Naz, I., 2022. A critical review on the phytoremediation of heavy metals from environment: performance and challenges. Chemosphere 291, 132979.
Singh, V.K., Singh, R., Rajput, V.D., Singh, V.K., 2023. Halophytes for the sustainable remediation of heavy metal-contaminated sites: recent developments and future perspectives. Chemosphere, 137524.
Syed, K., Tiwari, S., Sikka, J., Panwar, K., 2008. Impact of air pollution on floral morphology and characteristics of *Cassia glauca* Lamk. In Indore (India). J. Environ. Res. Dev. 3 (9), 91–96.
Team, R.C., 2023. R: A Language and Environment for Statistical Computing. R Foundation for Statistical Computing, Vienna, Austria.
Teranishi, Y., Tanaka, A., Osumi, M., Fukui, S., 1974. Catalase activities of hydrocarbon-utilizing *Candida* yeasts. Agric. Biol. Chem. 38 (6), 1213–1220.
Thakur, S., Singh, L., Zularisam, A.W., Sakinah, M., Din, M.F.M., 2017. Lead induced oxidative stress and alteration in the activities of antioxidative enzymes in rice shoots. Biol. Plant. (Prague) 61, 595–598.

Tiryakioglu, M., Eker, S., Ozkutlu, F., Husted, S., Cakmak, I., 2006. Antioxidant defense system and cadmium uptake in barley genotypes differing in cadmium tolerance. J. Trace Elem. Med. Biol. 20 (3), 181–189.
Truchet, D.M., Negro, C.L., Buzzi, N.S., Mora, M.C., Marcovecchio, J.E., 2023. Assessment of metal contamination in an urbanized estuary (Atlantic Ocean) using crabs as biomonitors: a multiple biomarker approach. Chemosphere 312, 137317.
Van der Ent, A., Baker, A.J., Reeves, R.D., Pollard, A.J., Schat, H., 2013. Hyperaccumulators of metal and metalloid trace elements: facts and fiction. Plant Soil 362 (1), 319–334.
Van Osten, M.J., Maggio, A., 2015. Functional biology of halophytes in the phytoremediation of heavy metal contaminated soils. Environ. Exp. Bot. 111, 135–146.
Veličković, M.V., 2010. Reduced developmental stability in *Tilia cordata* leaves: effects of disturbed environment. Period. Biol. 112 (3), 273–281.
Vujić, V., Avramov, S., Tarasjev, A., Barišić, K.N., Živković, U., Miljković, D., 2015a. The effects of traffic-related air pollution on the flower morphology of *Iris pumila* comparison of a polluted city area and the unpolluted deliblato sands (nature reserve). App. Ecol. Environ. Res. 13 (2), 405–415.
Vujić, V., Rubinjoni, L., Selaković, S., Cvetković, D., 2015b. Geometric morphometric examination of small-scale variations in leaf shape caused by anthropogenic disturbance in dioecious forest forb *Mercurialis perennis*. App. Ecol. Environ. Res. 13 (2), 405–415.
Wu, H., Liu, X., Zhao, J., Yu, J., 2013. Regulation of metabolites, gene expression, and antioxidant enzymes to environmentally relevant lead and zinc in the halophyte *Suaeda salsa*. Plant Growth Regul. 32, 353–361.
Yang, L., Wang, J., Yang, Y., Li, S., Wang, T., Oleksak, P., Kuca, K., 2022. Phytoremediation of heavy metal pollution: hotspots and future prospects. Ecot. Environ. Saf. 234, 113403.
Zar, J.H., 1999. Biostatistical Analysis. Prentice-Hall, Upper Sadle River, NJ, USA.
Zelditch, M., Swiderski, D., Sheets, H., Fink, W., 2004. Geometric Morphometrics for Biologists: a Primer. Elsevier Academic Press London, United Kingdom.
Zhao, F.J., Lombi, E., Breedon, T.M.S.P., 2000. Zinc hyperaccumulation and cellular distribution in Arabidopsis halleri. Plant Cell Environ. 23 (5), 507–514.
Zulfiqar, U., Farooq, M., Hussain, S., Maqsood, M., Hussain, M., Ishfaq, M., Anjum, M.Z., 2019. Lead toxicity in plants: impacts and remediation. J. Environ. Manage. 250, 109557.